Insights into the effect of ketylimine, aldimine, and vinylene group attachment and regiosubstitution on the fluorescence deactivation of fluorene

Stéphane Dufresne, Thomas Skalski, and W.G. Skene

Abstract: The spectroscopic and electrochemical properties of a 9-substituted fluorene ketylimine (**3**) were investigated and compared with those of its vinylene analogue (**4**) to determine the origins of the quenched fluorescence of these compounds. The predominate mode of singlet excited state deactivation of the heteroatomic fluorene was found to be internal conversion involving bond rotation. Meanwhile, its carbon counterpart was found to undergo deactivation preferentially by intersystem crossing to form its triplet, which was confirmed by laser flash photolysis. Both **3** and **4** quenched the fluorescence of fluorene with diffusion-controlled rate constants, implying that the singlet excited states of **3** and **4** are also quenched by intramolecular photoinduced electron transfer (PET). This deactivation mode was found to be exergonically favorable (–90 kJ/mol for **3** and –81 kJ/mol for **4**) according to the Rehm–Weller equation. The position of the heteroatomic bond on the fluorene moiety was further found to influence the singlet excited state deactivation pathway. The 2-substituted regioisomer decayed predominately by intramolecular PET and its fluorescence can be restored by acid protonation. Conversely, the PET mechanism is a minor deactivation mode for the 9-substituted fluorene derivative and its fluorescence can be enhanced by suppressing bond rotational modes, possible at low temperature and potentially in thin films.

Key words: fluorenyl ketylimines, intramolecular photoinduced electron transfer, Stern–Volmer quenching, azomethines.

Résumé : Afin de déterminer les origines de la fluorescence dégénérée de ces composés, on a étudié les propriétés spectroscopiques et électrochimiques des cétylimines de fluorènes portant un substituant en position 9 (**3**) et on les a comparées à celles de son analogue vinylène (**4**). On a trouvé que le mode dominant de la désactivation de l'état singulet excité du fluorène hétéroatomique se produit par une conversion interne impliquant une rotation de liaison. On a trouvé par ailleurs que sa contrepartie carbonée subit une désactivation préférentielle par un croisement intersystème conduisant à la formation de son triplet, ce qui est confirmé par la photolyse laser éclair. Les composés **3** et **4** désactivent tous la fluorescence du fluorène avec des constantes de vitesse contrôlées par la diffusion impliquant que l'état singulet excité des composés **3** et **4** est aussi désactivé par un transfert d'électron photoinduit (TEP) intramoléculaire. On a trouvé que, suivant l'équation de Rehm–Weller, ce mode de désactivation est favorable d'un point de vue exorgonique (–90 kJ/mol pour **3** et –81 kJ/mol pour **4**). On a trouvé aussi que la position de la liaison hétéroatomique dans la portion fluorène influence aussi la voie de désactivation de l'état singulet excité. On a aussi observé que le régioisomère portant un substituant en position 2 se désactive d'une façon prédominante par un TEP intramoléculaire et que sa fluorescence peut être restaurée par protonation acide. Inversement, le mécanisme de TEP n'est qu'un mode mineur de désactivation pour les dérivés du fluorènes portant un substituant en position 9 pour lesquels la fluorescence peut être augmentée par une suppression des modes de rotation des liaisons possibles à basse température et possiblement dans des films minces.

Mots-clés : cétylimines de fluorényles, transfert d'électron photoindut (TEP) intramoléculaire, désactivation de Stern–Volmer, azométhines.

[Traduit par la Rédaction]

Introduction

Conjugated materials have received much attention as a result of their photophysical and electrochemical properties, which make them suitable for organic electronics such as field-effect transistors, light-emitting diodes, and photovoltaics, to name but a few.[1–4] In particular, fluorene-based materials have been extensively studied because of their

Received 30 March 2010. Accepted 8 June 2010. Published on the NRC Research Press Web site at canjchem.nrc.ca on 13 January 2011.

This article is part of a Special Issue dedicated to Professor J. C. Scaiano.

S. Dufresne, T. Skalski,[1] and W.G. Skene.[2] Centre for Self-Assembled Chemical Structures, Département de Chimie, Université de Montréal, CP 6128, Centre-ville, Montreal, QC H3C 3J7, Canada.

[1]Present address: Université d'Artois, Unité de Catalyse et de Chimie du Solide, UMR CNRS n° 8181, Faculté Jean Perrin, rue Jean Souvraz, S.P. 18, 62307, Lens CEDEX, France.
[2]Corresponding author (e-mail: w.skene@umontreal.ca).

inherent high fluorescence, which makes them ideal for use in emitting devices.[5] Fluorene and its derivatives can additionally withstand the harsh oxidative and reductive environment of a device, further making them ideal materials for use in emitting devices.[6–8] Despite these advantages, the fluorescence quantum yield and color emitted by fluorene are highly sensitive to its environment and its substitution. This is evidenced by keto defects in the 9-position of fluorene, resulting in both decreased emission and undesired green emission.[6,9,10]

Although the fluorenone defect (**1**) (Chart 1) in polyfluorenes is undesired because it reduces device efficiency and results in color contamination, the ketone group is nonetheless interesting because it affords the means to introduce functionality into the conjugated fluorene polymer and to subsequently modulate the polymer's properties.[7,11–13] Simple condensation of amines with fluorene's ketone leads to ketylimines. The properties of the polyfluorenes such as solubility, electronic effects, color, and emission yields, to name but a few, can potentially be tailored by judicious choice of the amine used in preparing the ketylimine.

Despite the potential ease of preparing fluorene ketylimines such as **3** by simple condensation methods, few examples of these compounds are known.[14–16] Interestingly, no modern reports have described the successful synthesis of **3** or its derivatives, while only classic literature reports the preparation of some derivatives using harsh and extremely stringent reaction conditions.[17,18] The limited number of reports detailing the preparation of **3** and its derivatives, together with the absence of reported characterization, prompted us to prepare **3** to investigate the influence of the heteroatomic bond on the photophysical properties of fluorene. We were further incited to investigate the photophysical properties of both **3** and **4** by the lack of previous photophysical studies and by a desire to understand the origins of their unknown quenched fluorescence. The knowledge gained from investigating these model compounds is of importance not only for understanding the influence of the homo- and heteroatomic bonds on the photophysical properties, but also for designing and preparing future generations of fluorenyl compounds with tailored properties for specific applications. We additionally examined **3** because it is complementary to our previous aldimine studies of fluorene derivatives such as **5** and **6** and would provide vital structure–property information as well as information about the regiosubstitution effect on the photophysical properties.[19–24] The preparation and photophysical studies of **3** are therefore reported herein to understand the effect of the N=C group and its placement on the fluorenyl excited state properties.

Experimental procedures

General procedures

All reagents, including **1**, **2**, and **4**, were commercially available from Sigma-Aldrich and were used as received unless otherwise stated. Anhydrous and deaerated solvents were obtained with a Glass Contour solvent purification system. ^{1}H NMR and ^{13}C NMR spectra were recorded on a Bruker 400 MHz spectrometer with the appropriate deuterated solvents.

Chart 1.

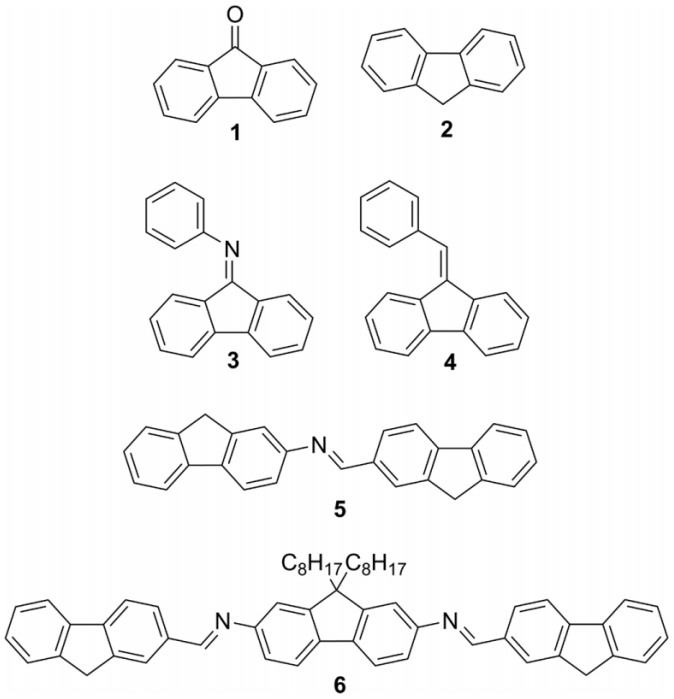

Spectroscopic measurements

The absorption measurements were done on a Cary 500 spectrometer, while the fluorescence studies were performed on an Edinburgh Instruments FLS-920 fluorimeter after deaerating the samples thoroughly with nitrogen for 20 min. Fluorescence absolute quantum yields were measured at 10^{-5} mol/L by exciting the compounds of study at the corresponding maximum absorption in spectroscopic grade dichloromethane at room temperature in an integrating sphere.[25] The ΔE values were calculated from the intercept of normalized absorption and fluorescence spectra of the corresponding compounds. The spectroscopic band gaps (E_g) were calculated from the tangent from the absorption onset.

Electrochemical measurements

Cyclic voltammetric measurements were performed on a Bioanalytical Systems EC epsilon potentiostat. Compounds were dissolved in anhydrous and deaerated dichloromethane at 10^{-4} mol/L with NBu_4PF_6 at sufficient concentration to achieve highly conductive solutions. A platinum electrode was used as the auxiliary and the working electrode, while a saturated Ag/AgCl electrode was used as the reference electrode. Ferrocene was added at the end of the analyses to serve as an internal reference. The electrochemical band gaps (E_g) were calculated from the measured oxidation and reduction potentials according to $E_{pa} + E_{pc} + 0.4$.

Laser flash photolysis

Laser flash photolysis experiments were done on a Luzchem mini-LFP system exciting at 355 nm with the third harmonic of a Nd-YAG laser. The solutions were prepared with matched absorbances between 0.3 and 0.5 at the excitation wavelength and deaerated for 20 min with nitrogen.

Highest occupied molecular orbital (HOMO) and lowest

unoccupied molecular orbital (LUMO) energy levels were calculated semiempirically using density functional theory (DFT) calculation methods available in Spartan 06 (Wavefunction, Inc.) with the 6-31g* basis set. The bond angles, distances, torsions, and other parameters were experimentally derived from the X-ray data from the corresponding structures.

N-*(9H-Fluoren-9-ylidene)benzenamine (3)*

Aniline (153 mg, 1.64 mmol) was dissolved with DABCO (500 mg, 4.45 mmol) in anhydrous toluene at 0 °C. This was followed by the slow addition of 1.0 mol/L $TiCl_4$ solution in toluene (2.77 mL, 2.77 mmol). Compound **1** (100 mg, 0.55 mmol) was added and then refluxed for 3–4 h. The solvent was removed and the product was isolated as a yellow solid after purification by recrystallization in 50:50 dichloromethane/hexanes or by flash chromatography on alumina with neat hexanes with 1% triethylamine increased to hexanes/ethyl acetate (95:5) (57 mg, 41%); mp 92–94 °C. ^{1}H NMR (acetone-d_6) δ: 7.85 (d, 1H, J = 7.6 Hz), 7.77 (m, 2H), 7.52 (m, 1H), 7.43 (m, 4H), 7.21 (m, 1H), 6.98 (m, 2H), 6.55 (d, 1H, J = 8.0 Hz). ^{13}C NMR (acetone-d_6) δ: 164.0, 153.9, 145.6, 143.6, 139.4, 139.3, 133.9, 132.7, 131.2, 130.7, 130.3, 130.0, 129.5, 128.5, 127.1, 125.7, 124.8, 122.4, 121.8, 119.7.

Crystal structure determination

Diffraction data for **3** were collected on a Bruker FR591 diffractometer using graphite-monochromatized Cu Kα radiation (1.54178 Å). The structures were solved by direct methods (SHELXS97, University of Göttingen). All nonhydrogen atoms were refined based on Fobs2 (SHELXS97, University of Göttingen), while hydrogen atoms were refined on calculated positions with fixed isotropic U, using riding model techniques.

Synthesis

Given the limited experimental protocols for the preparation of **3** and the lack of its detailed characterization, we set out to prepare this compound. We first attempted to prepare **3** via our previously successful methods for aldimines by simple condensation of **2** with aniline in absolute ethanol and in neat aniline.[26–28] Although some desired product was detected by both TLC and crude NMR, purification by standard methods yielded insufficient material for characterization and photophysical studies. The low yield is most likely a result of reduced reactivity because of steric hindrance of the ketone, while the product formed was most likely extremely hydrolytically sensitive and subsequently decomposed with standard chromatographic preparative methods.[14,17,29,30] The latter is supported by the absence of isolated products after silica gel chromatography. Stringent reaction protocols using $TiCl_4$ and an excess of DABCO were used for activating the hindered ketone and preventing imine hydrolysis, respectively. Product isolation was possible by column chromatography over activated basic alumina. Alternatively, the desired product could also be obtained by recrystallization of the crude reaction mixture from a 50:50 dichloromethane/hexanes mixture. We also attempted to prepare an aliphatic derivative of **3** using butylamine to understand the photodeactivation modes of the N=C bond with a limited degree of conjugation on the fluorophores. However, the desired product could not be obtained despite the various reaction conditions employed. Its instability is most likely a result of its extreme sensitivity to hydrolysis and it spontaneously decomposes under ambient conditions. Nonetheless, the unprecedented and complete characterization by standard methods confirmed the formation of **3** in high purity and sufficient amounts for spectroscopic measurements, albeit in low yield.

X-ray crystallographic data

Unlike aldimines, ketylimines lack the characteristic imine peak, allowing for unequivocal product identification by ^{1}H NMR. The lack of characteristic proton resonance at 8.5 ppm makes product identification challenging. Undeniable evidence for correct product formation is, however, possible by X-ray diffraction. In addition to this, the relation of the phenyl unit to the fluorene moiety can be determined from the X-ray diffraction data, allowing for comparison of the structures with analogous aldimines such as **6**.

Compound **3** was crystallized by slow evaporation from a saturated solution of acetone to give small yellow plates. The resolved structure (Fig. 1, left panel) confirms that **3** was formed and crystallizes in an orthorhombic unit as per Table 1. Three different molecules of **3** were found within the crystal lattice for a total of 24 molecules per lattice. Despite the large number of different molecules per lattice, only small variances were found between them. As seen in the right panel of Fig. 1, depicting the crystal structure shown along the *b*-axis, the phenyl moiety is not coplanar with the fluorene moiety. In fact, the planes described by the two aromatic moieties are twisted by 70°, 80°, and 85° for each of the three distinct molecules isolated per lattice. The twisting between the two planes is required to minimize the steric hindrance between the ortho protons of the phenyl and fluorene units. This is evident from the calculated HOMO and LUMO energy levels seen in Fig. 2 using the X-ray crystallographic data for the optimized geometry. It should be noted that the observed twisting between the two planes is greater than that for its aldimine regioisomer (**6**), whose two terminal fluorenes are twisted by 26° and 65° relative to the central fluorene.[24] Although the mean plane angles differ for **3** and its regioisomer (**6**), the corresponding bond distances and angles for the two analogues are identical within experimental error. The large twisting angle between the aromatic units nonetheless implies not only that the 9-position of the fluorene is sterically hindered, but that **3** has a limited degree of conjugation extending only through the fluorene=N portion. The latter is supported spectroscopically (vide infra). The severe steric hindrance and the large twisting of the fluorenyl and phenyl mean plane angles observed from the crystallographic data for **3** prevent any higher ordered structure arising from intermolecular interactions. In fact, the three-dimensional crystal network of **3** is governed by only weak face-to-π interactions. This is in contrast to **6**, which has a high degree of 3D ordering owing to many intermolecular π-stacking and C–H–π interactions.

Fig. 1. ORTEP X-ray structure of **3** with the ellipsoids shown at 50% probability along the *a*-axis (left) and *b*-axis (right).

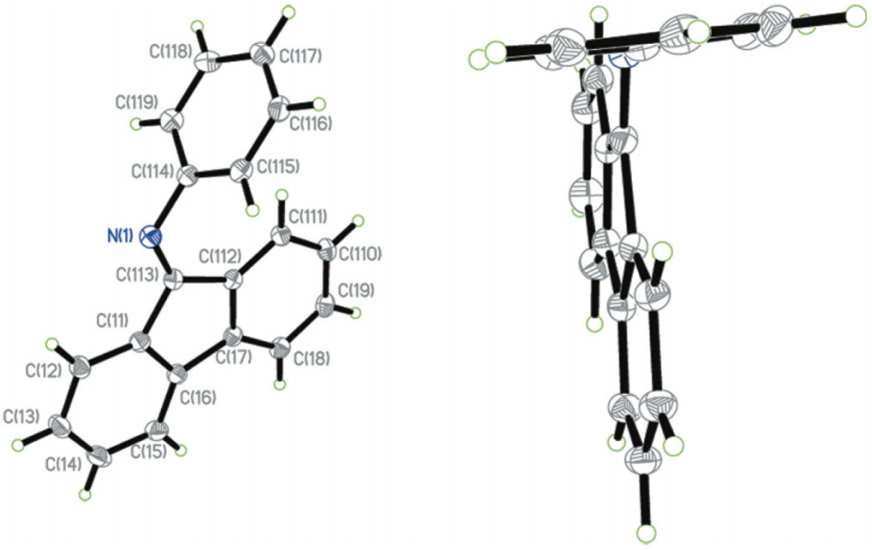

Table 1. Details of crystal structure determination for **3**.

	Compound **3**
Formula	$C_{19}H_{13}N$
M_w (g/mol); $F(000)$	255.30; 3216
Crystal color and form	Yellow plate
Crystal size (mm)	0.15 × 0.13 × 0.05
T (K); $D_{calcd.}$ (g/cm^3)	150(2); 1.247
Crystal system	Orthorhombic
Space group	*Pbca*
Unit cell	
a (Å)	9.6721(2)
b (Å)	16.4370(3)
c (Å)	51.3027(10)
α (°)	90.000
β (°)	90.000
γ (°)	90.000
V (Å^3); Z	8156.1(3); 24
θ range (°); completeness	1.76–72.26; 0.996
Reflections: collected/independent; R_{int}	8022/7112; 0.041
μ (mm^{-1})	0.556
Abs. corr.	Semiempirical
$R_1(F)$; $wR(F^2)$ [$I > 2\sigma(I)$]	0.0571; 0.1549
$R_1(F)$; $wR(F^2)$ (all data)	0.0629; 0.1580
GoF (F^2)	1.297
Max. residual e density (e Å^{-3})	–0.426

Spectroscopy

Given the limited reports examining the fluorescence of **3** and its analogous vinylene derivative (**4**),[31–33] we examined the photophysical properties of these two compounds. Such studies are required to understand the effect and the placement of the heteroconjugated bond on the fluorescence and the origin of the weak fluorescence of these compounds. This is possible by comparing the spectroscopic properties of **3**–**5**. As seen in Table 2, the three compounds exhibit approximately the same absorption maxima and differ only in their long wavelength absorption. The same trend of spectral shifts as a function of structures is also observed for their fluorescence spectra. It can be concluded from the absorption and fluorescence spectra of **3** and **4** that the heteroconjugated fluorene is more conjugated than its all-carbon counterpart. This is further supported by the shorter N=C bond distance (1.279 Å) compared with the corresponding C=C bond distance (1.340 Å) for **4**, derived from the X-ray crystallographic data. The shorter bond distance implies a greater sp^2 character to the bond and hence a higher degree of conjugation, which is further corroborated by the band gaps (E_g).

Both **3** and **4** possess substantially lower fluorescence quantum yields than **1** in dichloromethane, as seen in Table 2. More specifically, **4** does not fluoresce, while **3** only weakly fluoresces at room temperature. To better understand the origins of the differences between the two analogues and their quenched fluorescence relative to **1**, the fluorescence at 77 K was measured. All modes of rotational deactivation are suppressed at this temperature and an observed fluorescence increase would denote internal conversion deactivation by bond rotation. The fluorescence yield of **3** increased to 0.6 at 77 K, while no change was observed for **4** at this low temperature. Although an accurate ratio between the emission at 77 K and that at room temperature cannot be determined owing to the weak room temperature fluorescence, it can nonetheless be confirmed that the major mode of singlet excited state deactivation of **3** is by nonradiative means involving bond rotation, most likely the N–phenyl bond. Meanwhile, the singlet excited state deactivation of **4** occurs by other means. It can be concluded from the temperature fluorescence measurements that deactivation of excited fluorene is highly influenced by its substituents. This is evident from the temperature-dependent fluorescence of the regioisomers **3** and **4**, where two different deactivation modes occur despite the vinylene and imine bonds being isoelectronic. The different effect of the homoaryl and heteroconjugated bonds on the fluorene properties is further evidenced from the calculated HOMO and LUMO levels for **3** and **4**. As seen in Fig. 2, the HOMO is localized exclusively over the phenyl–N moiety and the LUMO is distributed across the fluorenyl moiety for **3**. This is in contrast to **4**, whose HOMO is distributed across the fluorenyl moiety while the

Fig. 2. HOMO (left) and LUMO (right) energy levels of **3** calculated using the DFT 6-31g* basis set using the X-ray crystallographic data for the optimized geometry.

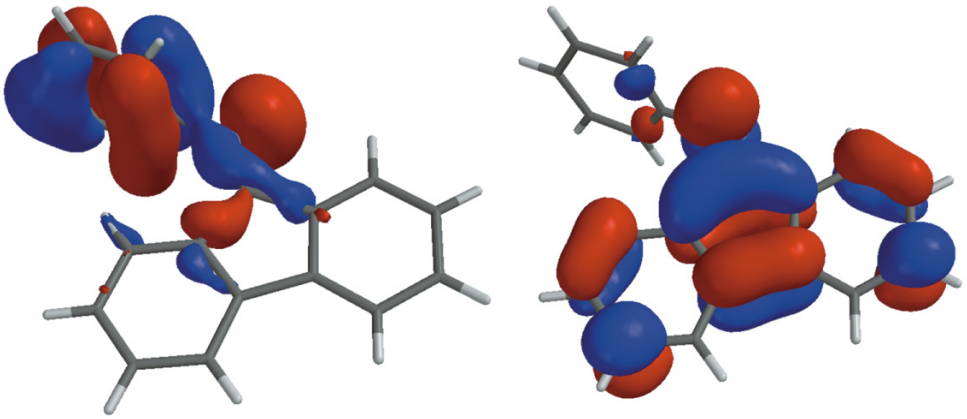

Table 2. Various spectroscopic data.

Compound	Absorbance (nm)[b,c]	Fluorescence (nm)[b]	ΔE (eV)	E_g spec (eV)	Fluorescence quantum yield[a] CH_2Cl_2	CH_2Cl_2 + TFA	77 K / RT[d]
1	258 (377)	505	2.9	3.6	0.02	0	7
2	261	302	4.4	3.9	0.50	0.45	4
3	258, 298 (388)	478	2.8	2.6	0.04	0.03	15
4	259 (328)	402	3.4	3.1	0	0	0
5[e]	361	445	2.9	2.9	0.40	—	—

[a]Absolute fluorescence quantum yield measured using an integrating sphere.

[b]Measured in CH_2Cl_2.

[c]Values in parentheses denote the most bathochromically shifted absorption maximum.

[d]Fluorescence quantum yield ratio measured at 77 K in a 4:1 methanol/ethanol matrix and at room temperature (RT) in methanol. The change in refractive index is minimal for the two temperatures, and therefore no temperature-dependent fluorescence correction is required.

[e]Ref. 21.

Fig. 3. HOMO (left) and LUMO (right) energy levels of **4** calculated using the DFT 6-31g* basis set using the X-ray crystallographic data for the optimized geometry.

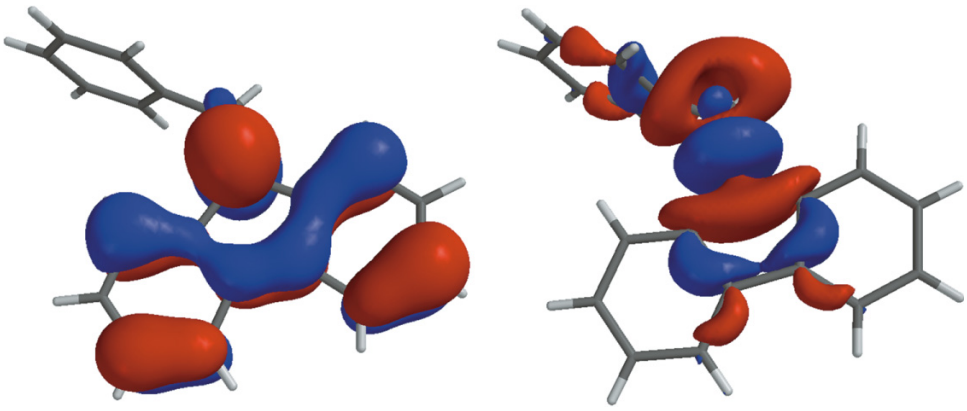

LUMO covers the cyclopentyl, imino, and phenyl moieties (Fig. 3).

The nonexistent room temperature fluorescence and the absence of increased fluorescence at a reduced temperature of **4** would suggest the presence of deactivation modes other than internal conversion. A possible deactivation mode would be intersystem crossing to form the triplet state. Both **3** and **4** were therefore further investigated by laser flash photolysis to spectroscopically confirm the formation of a triplet state. As seen in Fig. 4, a strong transient signal is apparent at 450 nm for the excitation of **4** at 355 nm by laser flash photolysis. The quenching of this transient with 1,3-cyclohexadiene and the unimolecular decay confirm the triplet nature of the transient. The similar transient intensities observed for optically matched samples of xanthone and **4** suggest that the triplet quantum yield of **4** is similar to that of xanthone ($\Phi_{TT} = 1$).[34–37] Conversely, no transient signal was detected for **3**, implying the absence of triplet

Fig. 4. Transient absorption spectra of xanthone (black) and **4** (red) measured at 0.12 μs after the 355 nm laser pulse in deaerated dichloromethane. Inset: monoexponential decay of transient **4** monitored at 450 nm.

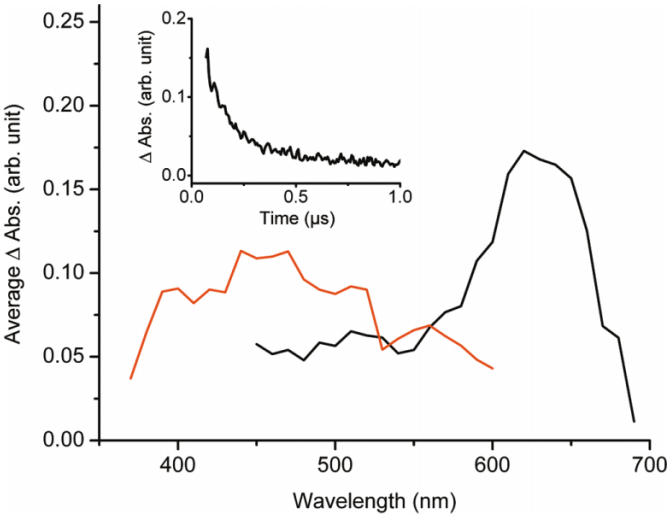

Fig. 5. Stern–Volmer fluorescence quenching of **2** with 0 (black), 20 (red), 40 (green), 60 (blue), and 80 (orange) mmol of **3** in dichloromethane. Inset: change in fluorescence of **2** with the addition of **3**, monitored at 318 nm.

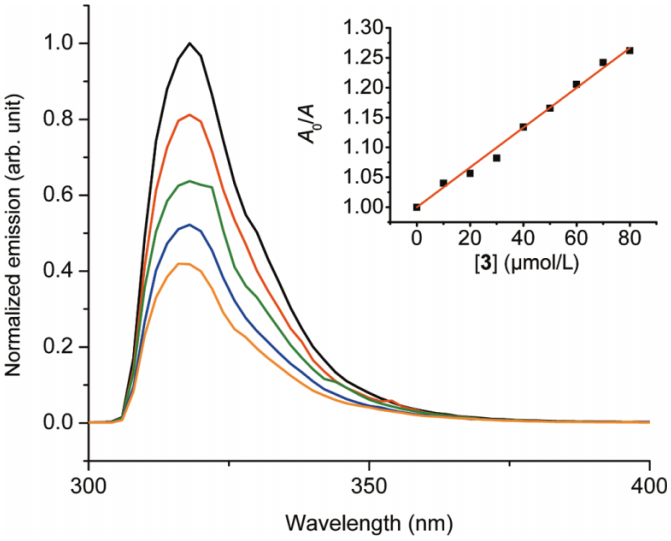

formation and hence no deactivation by intersystem crossing for the heteroatomic compound. The time-resolved and steady-state spectroscopic methods confirm that **3** preferentially deactivates by internal conversion, while the singlet excited state of **4** is predominately deactivated by intersystem crossing.

Although the temperature-dependent fluorescence confirms that the singlet excited state of **3** deactivates by internal conversion, the quantum yield of this process cannot be accurately measured. This is a result of the large error associated with comparing the intense fluorescence signal at 77 K with the extremely weak room temperature signal. Therefore, internal deactivation modes other than rotational internal conversion energy dissipation, such as photoinduced electron transfer (PET), cannot be dismissed. Stern–Volmer quenching studies of **3** and **4** were subsequently undertaken to determine whether other modes of singlet excited state deactivation occurred.[38] Owing to the quenched fluorescence of **3** and **4**, quantitative and accurate quenching studies were not possible using these two compounds as fluorophores. The quenching measurements were therefore done with fluorophore **2** because of its inherent high fluorescence yield. As seen in Fig. 5, **3** quenches the fluorescence of **2** with a bimolecular quenching rate constant (k_q) of 3.3×10^{11} L mol^{-1} s^{-1}, from the measured fluorescence lifetime of **2** (τ_o = 10 ns). Similarly, **4** also quenches **2** with $k_q = 4.0 \times 10^{11}$ L mol^{-1} s^{-1}. Higher quenching ratios of ϕ_o/ϕ would be beneficial to derive accurate k_q values. However, these were not possible because of spectroscopic screening effects of the quenchers at higher concentrations leading to deviations from linearity of the Stern–Volmer plots. The rate constants measured are slighter greater than the diffusion-controlled limit in dichloromethane ($k_q = 2 \times 10^{10}$ L mol^{-1} s^{-1}).[38] This is a result of overlapping absorbances between the fluorophore and the quencher at the excitation wavelength making it difficult to make accurate quenching measurements. Nonetheless, the calculated diffusion-controlled k_q confirm that the fluorene singlet excited state is efficiently deactivated by both **3** and **4**. The results are consistent with previous quenching studies of **1** with aliphatic imines that were deactivated by PET. The similarity of the quenching rate constants of **3** and **4** with their fluorophore-free quenching counterparts, concomitant with the favorable energetics (vide infra), implies that the singlet excited state deactivation occurs by intramolecular PET.[19–21]

The diffusion-controlled k_q quenching of **2** by both **3** and **4** implies deactivation by PET. The energetics of PET were empirically calculated according to the Rehm–Weller equation to corroborate the fluorescence quenching data: $\Delta G^\circ_{eT} = E_{pa}$ (fluorophore) – E_{pc} (quencher) – $\Delta E_{0,0}$ – λ.[39] The equation takes into account the fluorophore's oxidation potential (E_{pa}), the quencher's reduction potential by accepting the transferred electron from the fluorophore (E_{pc}), and the solvent reorganization energy (λ). The energy gap ($\Delta E_{0,0}$) between the ground and excited singlet states of **2** must also be taken into account, since PET involves electron transfer from the excited state. The required value is calculated from the intercept of the normalized plot of the absorption and fluorescence spectra of the fluorophores (see the Supplementary data). The E_{pa} and E_{pc} values (Table 3) were measured by cyclic voltammetry and correspond to the oxidation and reduction potentials of **2** and quenchers (**3** and **4**), respectively. The combined spectroscopic and electrochemical data (Tables 2 and 3) were used to calculate the energetics of PET. The exergonic values of –90 and –84 kJ/mol calculated for the quenching of **1** by **3** and **4**, respectively, support the Stern–Volmer quenching data and imply that deactivation of the singlet excited states of **3** and **4** also occurs by intramolecular PET. This deactivation mode is consistent with the 2-fluorenyl aldimine regioisomers that also deactivate by intramolecular PET.[19–21] Interestingly, the PET deactivation mode of 2-substituted regioisomers can be suppressed by protonating the azomethine, resulting in fluorescence yields near unity.[19–21] However, the fluorescence yield of **3** does not increase upon protonation (Table 2). This is most likely a result of the steric hindrance at the

Table 3. Electochemical data recorded in anhydrous and deaerated dichloromethane with a saturated Ag/Ag^+ reference electrode.

Compound	E_{pa} (eV)	E_{pc} (eV)	E_g (eV)
1	0.86	–1.03	2.3
2	0.91	–1.31	2.6
3	1.50	–1.40	3.3
4	1.73	–1.85	4.0

fluorenyl 9-position and as such, the imine cannot be efficiently protonated. Nonetheless, the spectroscopic and electrochemical data support the conclusion that the singlet excited states of **3** and **4** deactivate by intramolecular PET. While this degenerate manifold is also efficiently deactivated by rotational internal conversion in the case of **3**, **4** is efficiently deactivated predominately by intersystem crossing to form its triplet. The net outcome of these different deactivation processes is suppressed fluorescence for both **3** and **4**.

Conclusion

The origin of the previously unknown fluorescence suppression for 9-substituted fluorenes has been determined. Deactivation of the fluorophore excited state occurs by combined efficient rotational internal conversion and intramolecular photoinduced electron transfer for the heteroatomic ketylimine **3**. Although the singlet excited state of its carbon analogue (**4**) also deactivates by PET, the major mode of deactivation is by intersystem crossing resulting in efficient triplet formation. While the triplet manifold was spectroscopically confirmed by laser flash photolysis, evidence for the intramolecular PET mechanism was supported by examining the fluorescence rate constants for quenching of fluorene by both the ketylimine and vinylene fluorene derivatives. The PET mechanism was further supported by calculating the energetics according to the Rehm–Weller equation. Not only was the PET mechanism found to be exergonically favorable with these two quenchers, but deactivation of the singlet excited state occurred with diffusion-controlled rate constants. Unlike its 2-substituted fluorenyl regioisomers, the fluorescence of **3** cannot be restored by suppressing the PET mechanism by protonation. Nonetheless, the fluorescence quenching of **3** occurs predominately by rotational internal conversion, while that of its 2-substituted regioisomer occurs predominately by PET. The fluorescence of **3** can therefore be dramatically increased by reducing bond rotation deactivation modes, which is possible at low temperature or potentially in the solid state (e.g., by spin coating as thin films). The fluorescence enhancement possible with 9-heteroatomic fluorenyl imines makes these compounds beneficial and better suited for emitting devices than both their vinylene and 2-substituted regioisomer analogues, which waste their desired singlet excited state energy by uncontrollable means. Although the N=C bond is understood to be isoelectronic to the C=C bond, it was found that deactivation of the singlet excited state occurs by different modes depending on the type of unsaturated bond. The location of the N=C moiety on the fluorene was also found to play an important role in determining the fluorescence quenching mechanism. The future generation of materials for a given emitting or sensing application can therefore be prepared with the knowledge gained from the discovered fluorescence quenching mechanism.

Supplementary data

Supplementary data for this article are available on the journal Web site (canjchem.nrc.ca). CCDC 781760 contains the crystallographic data for this manuscript. These data can be obtained, free of charge, via www.ccdc.cam.ac.uk/conts/retrieving.html (or from the Cambridge Crystallographic Data Centre, 12 Union Road, Cambridge CB2 1EZ, UK; fax +44 1223 336033; or deposit@ccdc.cam.ac.uk).

Acknowledgements

The Natural Sciences and Engineering Research Council of Canada (NSERC) is thanked for a Discovery Grant, Strategic Research Grant, and Research Tools and Instruments grant allowing this work to be performed, and the Canada Foundation for Innovation (CFI) is thanked for additional equipment funding. W. G. S. also thanks the Royal Society of Chemistry for a JWT Jones Travelling Fellowship, thus allowing this manuscript to be completed. S. D. and T. S. thank NSERC and Le conseil général du Nord Pas de Calais and Le conseil municipal de Vaulx Vraucourt for graduate scholarships, respectively. T. S. also thanks the Direction des Relations Internationales of the Université de Montréal.

References

(1) Brédas, J.-L.; Norton, J. E.; Cornil, J.; Coropceanu, V. *Acc. Chem. Res.* **2009**, *42* (11), 1691. doi:10.1021/ar900099h. PMID:19653630.

(2) Bredas, J.-L.; Durrant, J. R. *Acc. Chem. Res.* **2009**, *42* (11), 1689. doi:10.1021/ar900238j. PMID:19916562.

(3) Kamtekar, K. T.; Monkman, A. P.; Bryce, M. R. *Adv. Mater.* **2010**, *22* (5), 572. doi:10.1002/adma.200902148. PMID: 20217752.

(4) Lee, K.; Nair, P. R.; Scott, A.; Alam, M. A.; Janes, D. B. *J. Appl. Phys.* **2009**, *105* (10), 102046. doi:10.1063/1.3116630.

(5) Grimsdale, A. C.; Chan, K. L.; Martin, R. E.; Jokisz, P. G.; Holmes, A. B. *Chem. Rev.* **2009**, *109* (3), 897. doi:10.1021/cr000013v. PMID:19228015.

(6) Chan, K. L.; Sims, M.; Pascu, S. I.; Ariu, M.; Holmes, A. B.; Bradley, D. D. C. *Adv. Funct. Mater.* **2009**, *19* (13), 2147. doi:10.1002/adfm.200990055.

(7) Jo, J.; Vak, D.; Noh, Y.-Y.; Kim, S.-S.; Lim, B.; Kim, D.-Y. *J. Mater. Chem.* **2008**, *18* (6), 654. doi:10.1039/b714138f.

(8) Rathnayake, H. P.; Cirpan, A.; Delen, Z.; Lahti, P. M.; Karasz, F. E. *Adv. Funct. Mater.* **2007**, *17* (1), 115. doi:10.1002/adfm.200600089.

(9) Montilla, F.; Mallavia, R. *Adv. Funct. Mater.* **2007**, *17* (1), 71. doi:10.1002/adfm.200600141.

(10) Romaner, L.; Pogantsch, A.; Scandiucci de Freitas, P.; Scherf, U.; Gaal, M.; Zojer, E.; List, E. J. W. *Adv. Funct. Mater.* **2003**, *13* (8), 597. doi:10.1002/adfm.200304360.

(11) Pijper, T. C.; Pijper, D.; Pollard, M. M.; Dumur, F.; Davey, S. G.; Meetsma, A.; Feringa, B. L. *J. Org. Chem.* **2010**, *75* (3), 825. doi:10.1021/jo902348u. PMID:20055375.

(12) Kappaun, S.; Scheiber, H.; Trattnig, R.; Zojer, E.; List, E. J. W.; Slugovc, C. *Chem. Commun. (Camb.)* **2008**, 5170. doi:10.1039/b808407f. PMID:18956058.

(13) Becker, K.; Lupton, J. M.; Feldmann, J.; Nehls, B. S.; Galbrecht, F.; Gao, D. Q.; Scherf, U. *Adv. Funct. Mater.* **2006**, *16* (3), 364. doi:10.1002/adfm.200500550.
(14) Suzuki, K.; Matsu-Ura, N.; Horii, H.; Sugita, Y.; Sanda, F.; Endo, T. *J. Appl. Polym. Sci.* **2002**, *83* (8), 1744. doi:10.1002/app.10101.
(15) Meng, Q.; Thibblin, A. *J. Am. Chem. Soc.* **1997**, *119* (6), 1224. doi:10.1021/ja9624681.
(16) Dai, W.; Srinivasan, R.; Katzenellenbogen, J. A. *J. Org. Chem.* **1989**, *54* (9), 2204. doi:10.1021/jo00270a034.
(17) O'Donnell, M. J.; Polt, R. L. *J. Org. Chem.* **1982**, *47* (13), 2663. doi:10.1021/jo00134a030.
(18) Pickard, P. L.; Tolbert, T. L. *Org. Synth.* **1964**, *5*, 51.
(19) Dufresne, S.; Pérez Guarìn, S. A.; Bolduc, A.; Bourque, A. N.; Skene, W. G. *Photochem. Photobiol. Sci.* **2009**, *8* (6), 796. doi:10.1039/b819735k. PMID:19492107.
(20) Dufresne, S.; Callaghan, L.; Skene, W. G. *J. Phys. Chem. B* **2009**, *113* (47), 15541. doi:10.1021/jp907391y.
(21) Bourque, A. N.; Dufresne, S.; Skene, W. G. *J. Phys. Chem. C* **2009**, *113* (45), 19677. doi:10.1021/jp907263p.
(22) Tsang, D.; Bourgeaux, M.; Skene, W. G. *J. Photochem. Photobiol. A* **2007**, *192* (2–3), 122. doi:10.1016/j.jphotochem.2007.05.013.
(23) Pérez Guarìn, S. A.; Skene, W. G. *Mater. Lett.* **2007**, *61* (29), 5102. doi:10.1016/j.matlet.2007.04.015.
(24) Guarìn, S. A. P.; Dufresne, S.; Tsang, D.; Sylla, A.; Skene, W. G. *J. Mater. Chem.* **2007**, *17*, (27), 2801. doi:10.1039/b618098a.
(25) Bolduc, A.; Dufresne, S.; Hanan, G. S.; Skene, W. G. *Can. J. Chem.* **2010**, *88* (3), 236. doi:10.1139/V09-166.
(26) Dufresne, S.; Skene, W. G. *J. Org. Chem.* **2008**, *73* (10), 3859. doi:10.1021/jo8002503. PMID:18410143.
(27) Guarìn, S. A.; Bourgeaux, M.; Dufresne, S.; Skene, W. G. *J. Org. Chem.* **2007**, *72* (7), 2631. doi:10.1021/jo070100o. PMID:17343421.
(28) Bourgeaux, M.; Skene, W. G. *J. Org. Chem.* **2007**, *72* (23), 8882. doi:10.1021/jo701515j. PMID:17956121.
(29) Saroja, G.; Pingzhu, Z.; Ernsting, N. P.; Liebscher, J. *J. Org. Chem.* **2004**, *69* (3), 987. doi:10.1021/jo035204n. PMID:14750836.
(30) Meng, Q.; Thibblin, A. *J. Am. Chem. Soc.* **1997**, *119* (6), 1224. doi:10.1021/ja9624681.
(31) Liao, W.-Y.; Wang, S.-S.; Yao, H.-H.; Chen, C.-W.; Tasi, H.-P.; Chu, W.-P.; Chen, J.-H.; Lee, S.-B. *IEEE Trans.* Magn. **2005**, *41*, 1019. doi:10.1109/TMAG.2004.842039.
(32) He, F.; Xia, H.; Tang, S.; Duan, Y.; Zeng, M.; Liu, L.; Li, M.; Zhang, H.; Yang, B.; Ma, Y.; Liu, S.; Shen, J. *J. Mater. Chem.* **2004**, *14* (18), 2735. doi:10.1039/b407262f.
(33) Liu, L.; Qiao, L.-X.; Liu, S.-Z.; Cui, D.-M.; Zhang, C.-M.; Zhou, Z.-J.; Du, Z.-L.; Wong, W.-Y. *J. Polym. Chem. A* **2008**, *46* (10), 3193. doi:10.1002/pola.22654.
(34) Carmichael, I.; Helman, W. P.; Hug, G. L. *J. Phys. Chem. Ref. Data* **1987**, *16* (2), 239. doi:10.1063/1.555782.
(35) Carmichael, I.; Hug, G. L. *J. Phys. Chem. Ref. Data* **1986**, *15* (1), 1. doi:10.1063/1.555770.
(36) Scaiano, J. C. *CRC Handbook of Organic Photochemistry;* CRC Press: Boca Raton, FL, 1989.
(37) Signals of identically matched intensity are not expected owing to the different triplet–triplet molar absorptivity coefficients of **4** and xanthone.
(38) Turro, N. J.; Ramamurthy, V.; Scaiano, J. C. *Principles of Molecular Photochemistry: An Introduction;* University Science Books: Sausalito, CA, 2009.
(39) Gilbert, A.; Baggott, J. *Essentials of Molecular Photochemistry;* CRC Press: Boca Raton, FL, 1991.